v1: 17 July 2026

Research Article

Long-Term Marine Thermal Signal in the El Jadida Coastal Region, Atlantic Morocco: A Climate Diagnostic Baseline for Gelidium Habitats and Coastal Resource Management

Preprinted: 8 May 2026
Peer-approved: 17 July 2026

© The Author(s) 2026. This is an Open Access article under the CC BY 4.0 license.

Qeios, Vol. 8 (2026)
ISSN: 2632-3834

Abdelatif Orbi[1], Jalal Annachat[2]

1. NOAMER, Morocco; 2. AR-WEB, Morocco

The El Jadida-Jorf Lasfar coastal region on the Moroccan Atlantic coast is influenced by seasonal upwelling and has socioeconomic relevance because of the exploitation of red seaweeds of the genus Gelidium. This study provides a climate-oriented diagnostic baseline of the marine thermal signal in this region and discusses its potential ecological relevance for Gelidium habitats, without treating sea surface temperature (SST) as a direct biological indicator of population status. Monthly SST series were extracted from NOAA OISST v2.1 for three points over 528 months from January 1982 to December 2025. Monthly climatologies, annual and seasonal trends, anomalies, period differences, and spatial contrasts were computed. The statistical analysis included ordinary least squares regression, confidence intervals, p-values, Mann-Kendall tests, and Sen slope estimates. Copernicus Marine SST was used as a higher-resolution spatial snapshot for February and August 2025, corresponding to cold- and warm-season reference months. A complementary daily MUR SST analysis was conducted for JJA 2016–2018 along three coastal-offshore transects (B-B′, D-D′, and F-F′), pairing offshore points with shallow coastal points located near the 20 m isobath.

Annual NOAA-based warming was detected at the three points, with trends of +0.095 °C decade^{-1} at B, +0.060 °C decade^{-1} at C, and +0.130 °C decade^{-1} at D. Warming was strongest in spring, whereas summer showed the weakest trends, particularly at the coastal point C, where the JJA trend was slightly negative. Copernicus snapshots confirmed that C was cooler than the offshore and near-offshore points, particularly in August 2025. The MUR daily analysis showed recurrent summer coastal cooling: the regional offshore-minus-coastal index was positive on 94.9% of JJA days during 2016–2018, and at least two of the three transects showed positive gradients on 92.0% of days. These results support the interpretation of a spatially structured thermal regime in which summer coastal cooling may be compatible with upwelling-related modulation. However, the analysis remains a surface thermal proxy and does not directly quantify upwelling intensity or Gelidium population responses. The study therefore provides a reproducible thermal baseline to support future

ecological monitoring and climate-informed management of Gelidium habitats and coastal marine resources.

Corresponding author: Abdellatif ORBI, orbi@noamermorocco.com

1. Introduction

The Atlantic coast of El Jadida, Morocco, belongs to a coastal domain influenced by seasonal upwelling. During the warm season, this process can bring colder and nutrient-rich waters toward the surface and the nearshore zone. This physical mechanism is well known locally: the waters of the Sidi Bouzid-El Jadida coastal sector may remain relatively cold during summer, sometimes reaching temperatures near 14 °C at the beach scale. Such a thermal regime gives the region a specific ecological and socioeconomic importance.

The El Jadida sector is part of the broader northeastern Atlantic and Canary Current upwelling context, where climate-driven changes can affect coastal thermal gradients, productivity, and ecosystem functioning. Climate change impacts on eastern boundary upwelling systems remain uncertain because warming, stratification, source-water changes, and upwelling intensity may interact in different ways[1]. In the Moroccan part of the Canary upwelling ecosystem, previous SST analyses have shown that warming can differ between coastal and oceanic locations and that such contrasts are related to upwelling intensity[2]. More recent work on the Moroccan Atlantic coast also supports the use of SST-based indices to monitor spatial and seasonal upwelling variability[3].

The region is also historically associated with the exploitation of red macroalgae of the genus Gelidium, a key raw material for agar production. Morocco, Portugal, and Spain have historically belonged to the main Atlantic areas where harvested Gelidium has supplied local agar producers[4]. Gelidium is especially relevant because commercial harvests are largely based on natural stocks and because the world agar market has experienced concerns related to the availability and sustainability of technical agar resources[5]. The sustainability of Gelidium habitats therefore depends not only on harvesting management but also on the evolution of physical conditions, particularly the thermal environment.

Recent trade statistics confirm that Morocco remains an important exporter of agar-agar, while avoiding any direct inference on local algal-bed status. For HS 130231 (agar-agar), WITS reports Moroccan exports in 2023 of USD 29.1 million, corresponding to 945,885 kg, with Japan, the United States, the United Kingdom, France, and India among the main destination markets[6]. The Moroccan Ministry of Industry and Trade also issues export notices for raw algae and agar-agar, confirming that this value chain is subject to export licensing and administrative allocation procedures[7]. These trade statistics are used here only to document the contemporary economic relevance of agarophyte resources and agar production; they are not interpreted as estimates of Gelidium biomass, local stock status, or the condition of the El Jadida algal beds.

This framing is also relevant from a planning perspective. Fishery and algal resource management plans are commonly structured around access, harvest levels, spatial allocation, and monitoring requirements, while the explicit integration of marine climate-change signals remains limited or uneven. The El

 doi.org/10.32388/OYZ6H3.2

Jadida Gelidium case is therefore used here as an emblematic coastal resource for which climate screening is needed, but the broader argument applies to fisheries management plans as a whole: future planning should incorporate thermal trends, seasonal anomalies, upwelling variability, and other climate-related indicators alongside conventional biological and socioeconomic information.

In this context, long-term SST analysis can provide a first diagnostic of the marine climate signal affecting the El Jadida coast. However, the interpretation must be cautious because regional satellite products may smooth nearshore gradients and because the response of Gelidium populations cannot be attributed to temperature alone. Biological and ecological studies show that Gelidium populations also respond to wave exposure, substrate availability, water clarity, nutrients, irradiance, sedimentation, local upwelling intensity, and harvesting pressure[8][9][10].

The aim of this paper is therefore to assess whether a long-term marine thermal signal is detectable in the El Jadida coastal region between 1982 and 2025, to examine its seasonal and spatial structure, to evaluate the surface expression of summer coastal cooling using a high-resolution MUR SST transect approach, and to discuss the potential ecological relevance of this signal for Gelidium habitats and climate-informed coastal resource management. The study is not designed as a direct biological assessment of Gelidium populations; rather, it establishes a physical thermal baseline that can guide future field-based ecological work.

2. Objectives

The study addresses four main questions. First, does the El Jadida region show a thermal signal compatible with background marine warming over the 1982–2025 period? Second, is this signal uniform across seasons, or is it moderated during summer by coastal cooling processes? Third, do the coastal, near-offshore, and offshore NOAA points show spatial contrasts that can help interpret the coastal thermal regime? Fourth, do high-resolution MUR daily transects show recurrent offshore-minus-coastal gradients during summer in the shallow coastal domain near the 20 m isobath?

Gelidium is retained as the ecological and socioeconomic context of the study because the El Jadida–Jorf Lasfar coast is historically linked to Gelidium harvesting and agarophyte resources. The analysis distinguishes between the documented SST patterns and the potential ecological relevance of those patterns. The ecological interpretation is therefore framed as hypothesis-generating and requires dedicated biological data on biomass, cover, recruitment, thallus condition, harvesting pressure, and habitat quality before any population-level conclusion can be drawn.

The study also uses a model-based environmental diagnostic framework. In this manuscript, the term model refers to the use of gridded satellite-derived/modeled SST products and statistical trend models applied to long-term time series. It does not refer to a biological population model of Gelidium. This distinction is important: the manuscript evaluates a marine climate signal and its planning relevance, while identifying the biological monitoring needed to test population-level responses.

doi.org/10.32388/OYZ6H3.2

3. Study Area and Data Sources

3.1. Study points

Three NOAA-based points were selected in the El Jadida coastal region to describe the regional coastal-offshore SST structure. Point B and point D were used as offshore or outer-shelf thermal reference points, while point C was used as the coastal SST reference point located closer to the shoreline and therefore more relevant for interpreting the surface thermal context of shallow coastal habitats. Point C should not be interpreted as a direct biological station for Gelidium; it is a satellite-based coastal surface-temperature reference within the limits of the product resolution.

Point	Coordinates	Approx. bathymetric setting	Analytical role
B	33.125°N; 8.875°W	Offshore / >50 m domain	Regional offshore reference
C	33.2360°N; 8.5741°W	Shallow coastal domain, near 20 m isobath	Coastal SST reference
D	33.2714°N; 8.6448°W	Offshore / outer-shelf domain	Near-offshore / offshore reference

Table 1. Geographic coordinates, approximate bathymetric setting and analytical role of points B, C and D.

3.2. Morpho-bathymetric setting and upwelling context

The El Jadida-Jorf Lasfar coastal sector is not morpho-bathymetrically uniform. Along this coastal stretch, two broad configurations can be distinguished. In some areas, the continental shelf is relatively narrow and the bathymetric contours are closely spaced, indicating a rapid transition from shallow coastal waters to deeper offshore waters. In such sectors, deeper and colder waters are located relatively close to the coastline, which may favor a sharper surface thermal response during upwelling-favorable periods. In contrast, other sectors show a wider and more gently sloping shelf, where the 20 m, 30 m and 50 m isobaths are located farther from the coast. These differences provide a physical context for interpreting the spatial expression of the SST signal, without implying that bathymetry alone controls upwelling.

Local professional knowledge indicates that Gelidium beds in the El Jadida-Jorf Lasfar sector are mainly associated with shallow rocky bottoms and are generally found within the upper coastal bathymetric range, approximately down to the 25 m isobath. Beyond about 30 m depth, Gelidium becomes absent or very scarce in the study area. Therefore, the 0-50 m bathymetric band is considered here as a broader coastal oceanographic domain, whereas the 0-25/30 m band represents the most relevant bathymetric range for the potential interpretation of Gelidium habitats.

Three additional paired transects were defined for the high-resolution MUR SST analysis: B-B′, D-D′ and F-F′. In each pair, the offshore point is compared with a shallow coastal point located near the 20 m isobath. This paired design allows

doi.org/10.32388/OYZ6H3.2

the daily surface thermal contrast between offshore waters and the shallow coastal domain to be analyzed within the same SST product.

Transect	Offshore point	Coastal point	Distance	Role
B-B′	B	B′ near 20 m	14.45 km	South-western coastal-offshore gradient
D-D′	D	D′ near 20 m	12.46 km	Central coastal-offshore gradient
F-F′	F	F′ near 20 m	17.45 km	North-eastern coastal-offshore gradient

Table 2. Paired transects used for the high-resolution MUR coastal-offshore thermal gradient analysis.

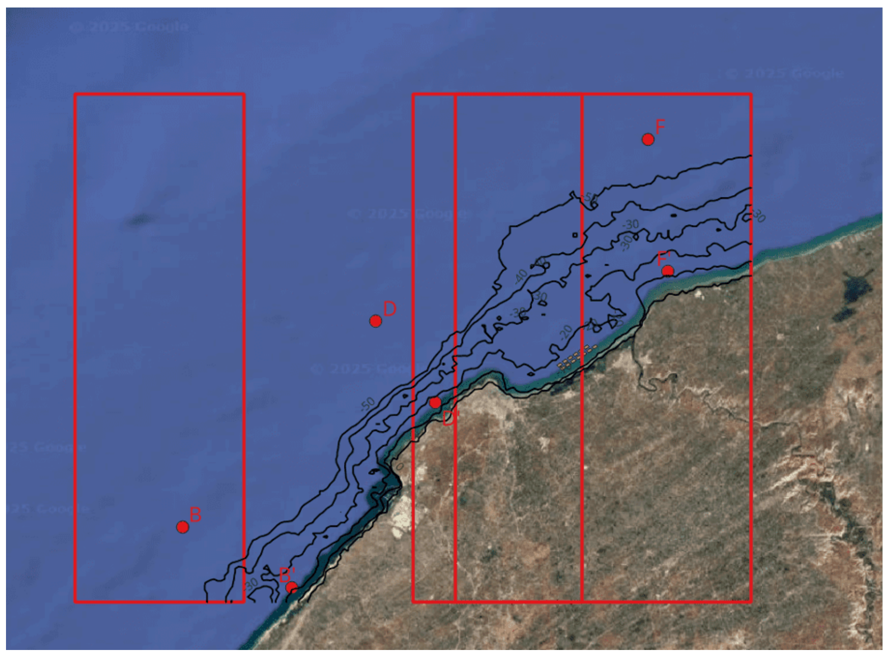

Figure 1. Location of the MUR coastal-offshore transects B-B′, D-D′ and F-F′ in relation to bathymetric contours and satellite SST grid cells/pixels. Offshore points B, D and F are paired with coastal points B′, D′ and F′ located around the 20 m isobath. The red rectangles represent the footprint/position of satellite SST grid cells or pixel windows used to assess spatial representativeness; they are not ecological boundaries or management zones.

The paired-transect map is used to document the spatial relationship between the offshore and shallow coastal points, the local bathymetry and the satellite SST grid structure. This is important because the MUR transects are used to quantify daily coastal-offshore SST gradients, whereas the NOAA grid is retained for long-term regional climate-scale analysis. The coastal points B′, D′ and F′

doi.org/10.32388/OYZ6H3.2

represent surface thermal references over the shallow bathymetric domain near 20 m; they are not direct biological sampling stations or near-bottom temperature measurements within Gelidium beds.

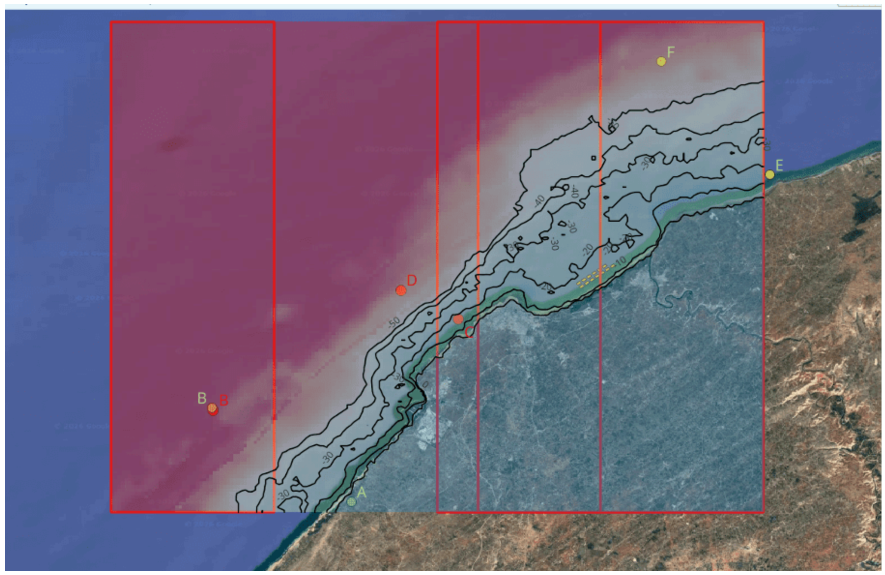

Figure 2. Study points, bathymetric contours and satellite SST grid-cell/pixel structure used to assess the spatial relationship between coastal and offshore references. The red rectangles show the satellite SST grid cells/pixel windows relative to the coastline and isobaths. They are included to illustrate the resolution constraint of gridded SST products and the position of the points relative to the pixels, not to delimit Gelidium habitats.

Historical INRH biomass-density survey maps were also considered to document the spatial relevance of the El Jadida coastal sector for *Gelidium* resources. These maps are used here only as contextual evidence of historically surveyed algal-resource areas, not as a quantitative assessment of current biomass or stock status.

doi.org/10.32388/OYZ6H3.2

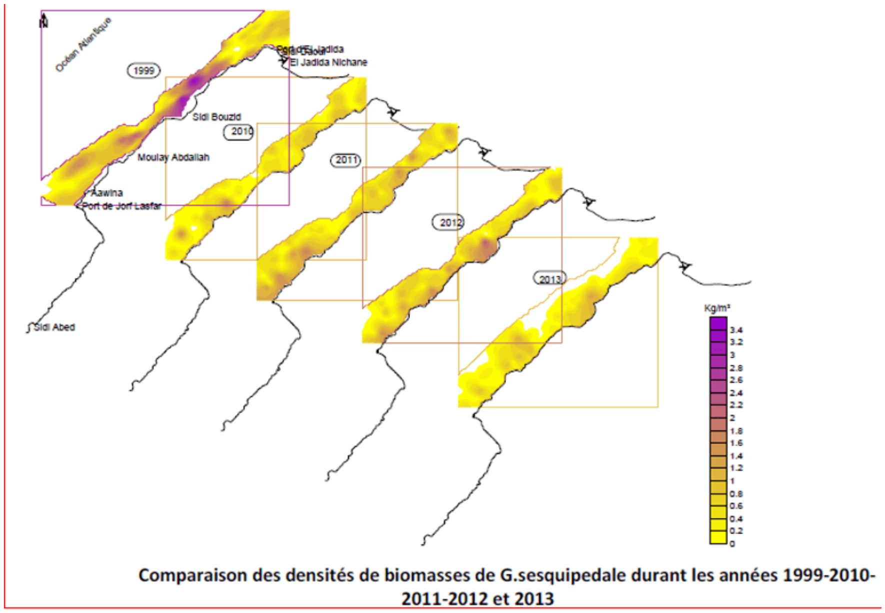

Figure 3. Historical INRH biomass-density survey areas for *Gelidium corneum* syn. *G. sesquipedale* in the El Jadida coastal sector. The colored survey bands document areas historically monitored for algal biomass density and are used in this study only to support the spatial relevance of the selected coastal sector. Source: INRH[11], Diagnostic de la récolte et de la valorisation des algues marines.

The figure supports the selection of the El Jadida-Jorf Lasfar coastal domain as a relevant sector for a climate-oriented SST baseline applied to shallow agarophyte habitats. It is not used to infer changes in algal biomass in the present study.

In Figures 1 and 2, the red rectangles are retained to make the gridded nature of the SST products visible. They indicate the satellite pixel/grid-cell context within which the point extractions are interpreted. This is important because the nearshore points are close to the coastline and to steep bathymetric gradients, where a single gridded SST value may integrate conditions over an area larger than the actual shallow coastal habitat.

3.3. NOAA OISST v2.1

The main long-term calculations were based on NOAA OISST v2.1[12][13]. This product provides global SST fields on a regular 0.25° grid and is suitable for climate-scale assessment. The useful monthly series extracted for this study cover 528 months, from January 1982 to December 2025, for each of the three NOAA points. Because the spatial resolution is coarse compared with the nearshore geometry of El Jadida and the bathymetric domain relevant to Gelidium, NOAA results are interpreted as regional-scale thermal indicators rather than fine-scale habitat measurements.

3.4. Copernicus Marine SST product

To complement the regional interpretation from NOAA, a higher-resolution Copernicus Marine product was used: SST_ATL_SST_L4_REP_OBSERVATIONS_010_026. This Atlantic reprocessed L4 SST product provides daily gap-free SST fields on a 0.05° grid. In this study, it was

doi.org/10.32388/OYZ6H3.2

used for targeted spatial interpretation around points B, C, and D for February 2025 and August 2025. These two months were selected because the NOAA climatology identifies February as the coldest month and August as the warmest month at the three study points. They are therefore interpreted as cold-season and warm-season high-resolution snapshots, not as a basis for inferring long-term Copernicus trends. The Copernicus product is used to examine whether a finer-resolution field reproduces the coastal-offshore contrast suggested by the NOAA-based analysis.

4. Methods

Let SST(y,m,p) be the monthly sea surface temperature for year y, month m, and point p. The monthly climatology was calculated as Clim(m,p) = (1/N) Σ SST(y,m,p), where N = 44 years for the 1982–2025 period. The annual mean was calculated as Ann(y,p) = (1/12) Σ SST(y,m,p). A linear trend was then fitted to the annual means and expressed in °C per decade.

Monthly anomalies were calculated as A(y,m,p) = SST(y,m,p) - Clim(m,p). Seasonal anomalies were then calculated for DJF, MAM, JJA, and SON as the mean of the three monthly anomalies within each season. DJF was handled as a cross-year season. Period differences were computed as ΔT(s,p) = mean anomaly in the recent period minus mean anomaly in the early period. The periods used were 1982–2000 and 2001–2025 for MAM, JJA, and SON, and 1983–2000 and 2001–2025 for DJF.

4.1. Statistical analysis and uncertainty treatment

Annual and seasonal trends were estimated using ordinary least squares regression and reported in °C decade^{-1}. For the main trend estimates, p-values, R^2 values, and 95% confidence intervals were calculated. The non-parametric Mann-Kendall test was applied to test monotonic tendencies, and the Sen slope was used as a robust trend-magnitude estimator. The statistical results are interpreted conservatively because SST series may exhibit serial autocorrelation and because the objective is to characterize an environmental baseline rather than to perform a formal attribution analysis.

4.2. High-resolution MUR coastal-offshore thermal-gradient analysis

To better assess the surface thermal expression of summer coastal cooling, a complementary high-resolution analysis was conducted using the MUR SST product. Unlike NOAA OISST, which was retained for the long-term regional climatology and trend analysis, MUR was used to examine daily coastal-offshore SST gradients at finer spatial resolution. Three paired transects were analyzed across the El Jadida–Jorf Lasfar coastal sector: B–B′, D–D′, and F–F′. In each pair, B, D, and F represent offshore reference points, while B′, D′, and F′ represent shallow coastal reference points located near the 20 m isobath. The analysis was conducted for JJA 2016–2018, based on daily MUR SST values.

For each daily MUR extraction, the calculation was performed in four successive steps. The equations are presented separately below to avoid ambiguity between point SST values, transect-specific indices, the regional index, and the normalized gradients.

Step 1 - Daily offshore-minus-coastal thermal contrast for each transect:

$$UI_B(d) = SST_B(d) - SST_B{}'(d)$$

$$UI_D(d) = SST_D(d) - SST_D{}'(d)$$

$$UI_F(d) = SST_F(d) - SST_F{}'(d)$$

where d is the day of observation. Positive values indicate that the coastal point is cooler than the offshore point on the same day.

Step 2 - Regional daily coastal-cooling index:

$$UI_{mean}(d) = [UI_B(d) + UI_D(d) + UI_F(d)]/3$$

Step 3 - Frequency of positive coastal-cooling situations:

$$F_{positive} = [N(UI > 0)/N_{total}] \times 100$$

Step 4 - Distance-normalized gradient:

$$G = UI/Distance$$

Distances used for normalization were 14.45 km for B-B′, 12.46 km for D-D′, and 17.45 km for F-F′.

5. Results

5.1. Monthly climatology

Month	B	C	D
January	17.34	17.19	17.35
February	16.77	16.66	16.78
March	16.85	16.79	16.88
April	17.62	17.59	17.67
May	19.01	19.02	19.10
June	20.83	20.87	20.99
July	21.83	21.86	22.12
August	22.33	22.32	22.72
September	22.17	22.05	22.50
October	21.25	21.06	21.47
November	19.62	19.40	19.77
December	18.22	18.02	18.28

Table 3. Monthly SST climatology at points B, C, and D over 1982–2025.

February was the coldest month at the three points, whereas August was the warmest month. The annual thermal amplitude, calculated as Tmax - Tmin, was 5.56 °C at B, 5.65 °C at C, and 5.94 °C at D. Point D therefore showed the largest annual amplitude. These climatological values are reported with limited decimal precision because the effective uncertainty of gridded SST products does not justify excessive numerical detail.

Point	Tmax (°C)	Tmin (°C)	Amplitude (°C)
B	22.33	16.77	5.56
C	22.32	16.66	5.65
D	22.72	16.78	5.94

Table 4. Annual thermal amplitudes at points B, C, and D.

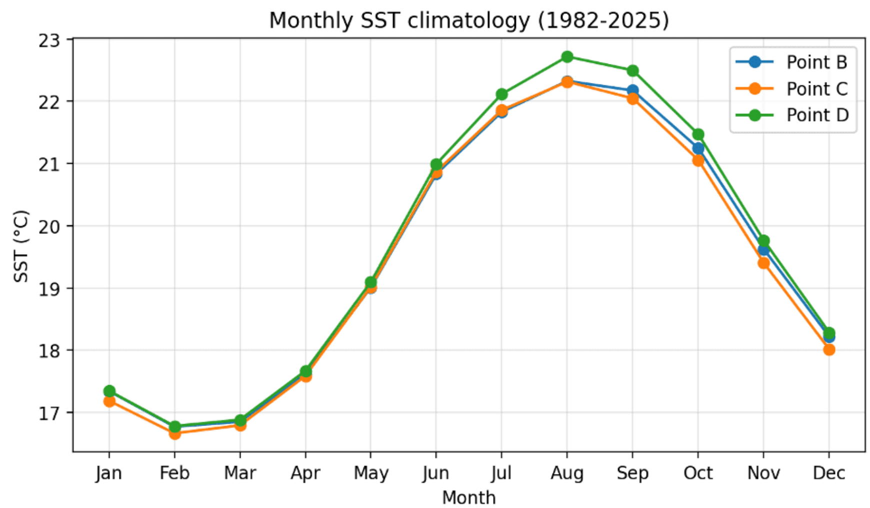

Figure 4. Monthly SST climatology at points B, C, and D over 1982–2025.

5.2. Annual evolution and trends

The annual mean SST showed a warming signal at the three points. The strongest trend was observed at D (+0.130 °C decade^{-1}), followed by B (+0.095 °C decade^{-1}), whereas the coastal point C showed the weakest trend (+0.060 °C decade^{-1}). The comparison between the first decade (1982–1991) and the last decade (2016–2025) confirms this hierarchy, with an increase of +0.39 °C at D, +0.29 °C at B, and +0.16 °C at C. The stronger warming at D is interpreted as offshore spatial heterogeneity or a possible front-related thermal behavior, but not as direct evidence of a displacement of the upwelling front.

doi.org/10.32388/OYZ6H3.2

Point	Trend (°C per decade)
B	+0.10
C	+0.06
D	+0.13

Table 5. Annual SST trends at points B, C, and D.

Point	1982–1991	2016–2025	Difference (°C)
B	19.34	19.62	0.29
C	19.29	19.45	0.16
D	19.44	19.84	0.39

Table 6. Comparison of annual mean SST between the beginning and the end of the series.

Figure 5. Interannual evolution of annual mean SST at points B, C, and D over 1982–2025.

doi.org/10.32388/OYZ6H3.2

5.3. Seasonal trends

Season	B	C	D
DJF	+0.15	+0.11	+0.15
MAM	+0.16	+0.15	+0.18
JJA	+0.01	−0.02	+0.10
SON	+0.08	+0.02	+0.11

Table 7. Seasonal SST trends at points B, C, and D.

Spring (MAM) was the season with the strongest warming at the three points. Summer (JJA) was the most stable season, especially at B and C. At point C, the JJA trend was slightly negative (–0.018 °C decade^{-1}). This result is compatible with a possible summer coastal-cooling modulation, potentially related to upwelling or nearshore mixing, but it should not be interpreted alone as statistical proof of a change in upwelling intensity.

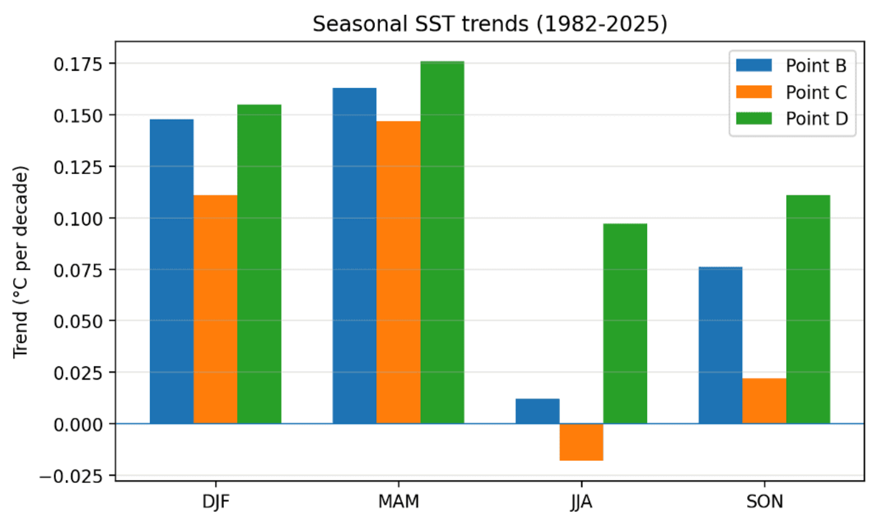

Figure 6. Seasonal SST trends at points B, C, and D over 1982–2025.

doi.org/10.32388/OYZ6H3.2

5.4. Mean differences between early and recent periods

Season	B	C	D
DJF	+0.26	+0.18	+0.26
MAM	+0.29	+0.27	+0.32
JJA	+0.07	+0.04	+0.25
SON	+0.37	+0.27	+0.43

Table 8. Mean thermal differences between early and recent periods.

The recent period was warmer than the early period in all seasons and at all points. The largest differences were found in SON and MAM. Point D again showed the strongest change, including in JJA, whereas point C remained comparatively more stable during the warm season.

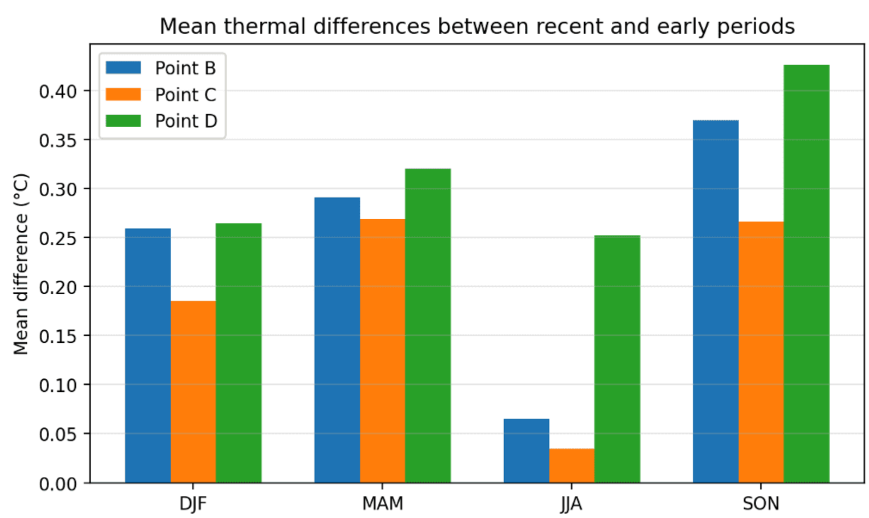

Figure 7. Mean thermal differences between early and recent periods at points B, C, and D.

doi.org/10.32388/OYZ6H3.2

5.5. Spatial comparison between B, C, and D

Season	B	C	D
DJF	17.44	17.29	17.47
MAM	17.83	17.80	17.88
JJA	21.66	21.68	21.94
SON	21.02	20.84	21.25

Table 9. Absolute seasonal mean SST at points B, C, and D.

The spatial structure was not uniform. In winter, C was cooler than B and D. In summer, D became warmer than both B and C, while B and C remained closer to each other. In autumn, C remained the coolest point and D the warmest. Because B and D both represent offshore or outer-shelf thermal references, their differences are interpreted as spatial heterogeneity within the offshore domain rather than as a direct ecological gradient. The main ecological contrast remains the difference between the coastal surface reference and the offshore thermal field.

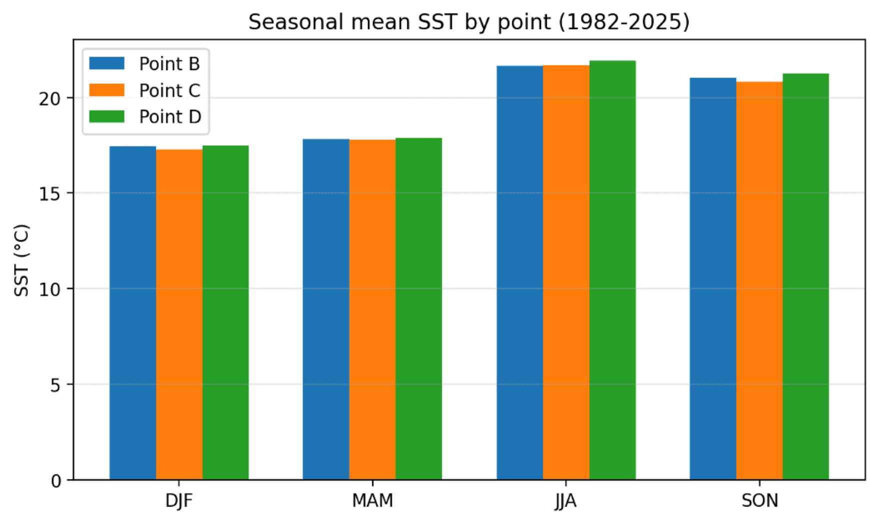

Figure 8. Seasonal mean SST by point over 1982–2025.

doi.org/10.32388/OYZ6H3.2

5.6. Complementary contribution of Copernicus Marine SST

Period	B	C	D
February 2025	17.34	16.89	17.19
August 2025	21.86	20.53	21.03

Table 10. Copernicus monthly mean SST extracted at points B, C, and D in February and August 2025.

The Copernicus extraction confirmed that the coastal point C was cooler than B and D in February 2025 and markedly cooler in August 2025. These two months should be interpreted as high-resolution cold-season and warm-season snapshots. They support the existence of a local coastal thermal gradient, but they do not by themselves establish a long-term spatial trend in the Copernicus product.

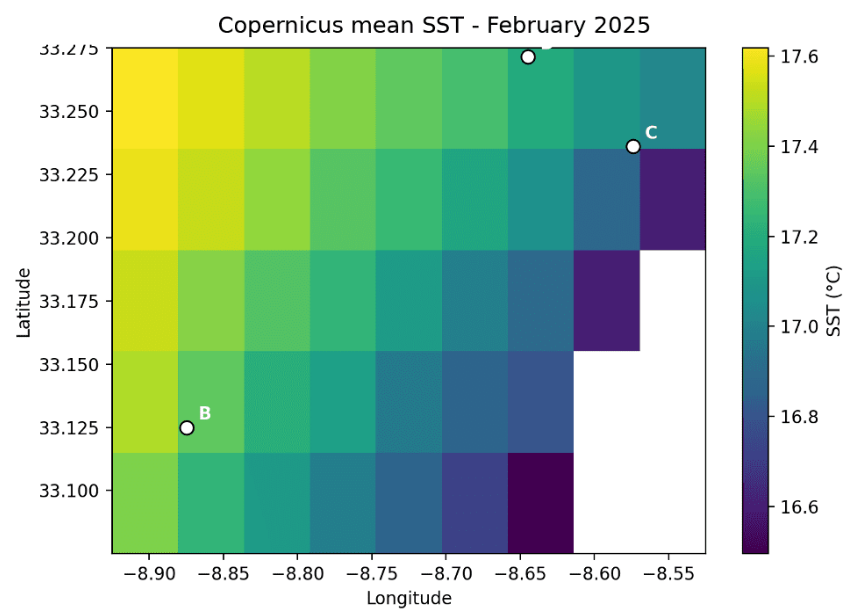

Figure 9. Copernicus SST field in February 2025, with points B, C, and D.

doi.org/10.32388/OYZ6H3.2

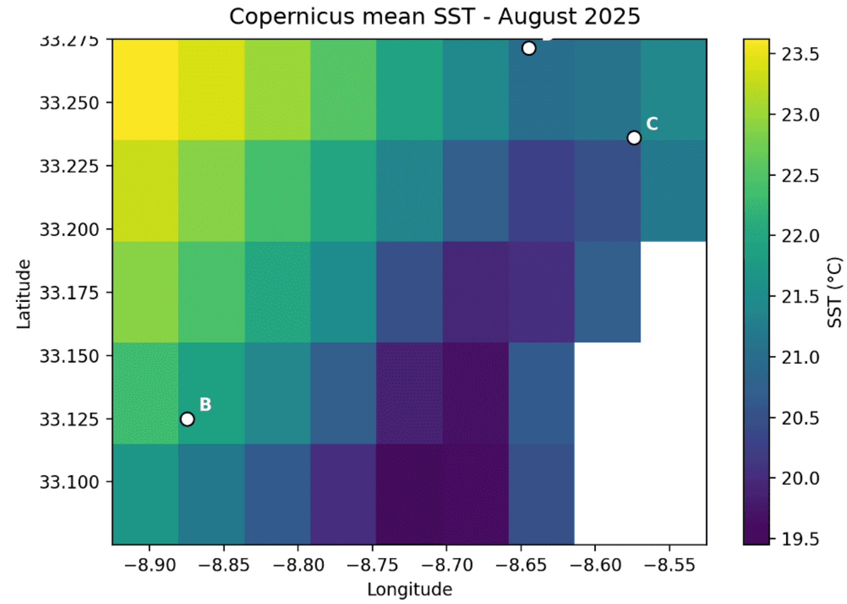

Figure 10. Copernicus SST field in August 2025, with points B, C, and D.

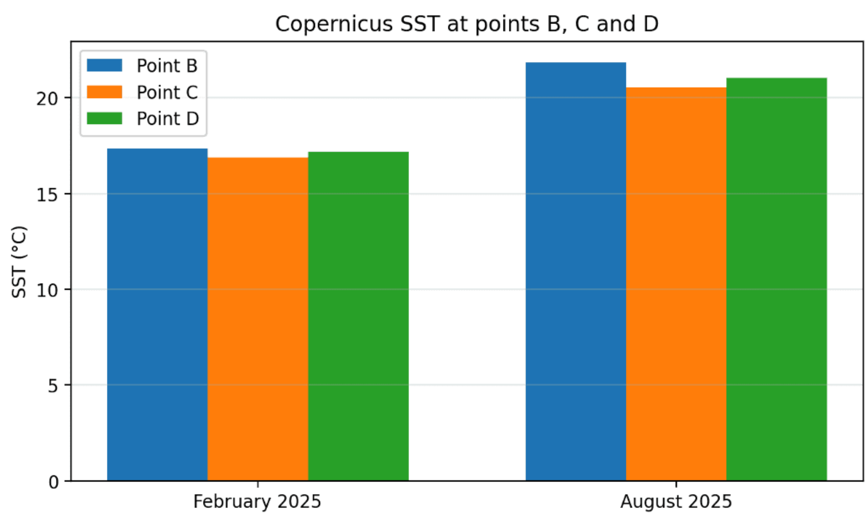

Figure 11. Direct comparison of Copernicus monthly mean SST at points B, C, and D in February and August 2025.

5.7. Robust trend statistics and uncertainty assessment

The statistical analysis confirms that the offshore point B shows a statistically supported warming signal over 1982–2025, while the coastal point C shows a weaker and less statistically robust annual signal. This difference is important because it supports the interpretation that nearshore thermal dynamics are not identical to offshore warming and may be modulated by upwelling, coastal mixing, or local oceanographic processes. The offshore-minus-coastal gradient also increases significantly through time, indicating that the offshore point has warmed more rapidly than the coastal reference over the period analyzed.

Series	n	OLS slope (°C/dec)	95% CI	OLS p	R^2	MK p	Sen slope (°C/dec)	Sen 95% CI
B (offshore)	44	0.095	[0.026; 0.164]	0.008	0.155	0.023	0.094	[0.015; 0.160]
C (coastal)	44	0.060	[−0.013; 0.134]	0.105	0.061	0.163	0.062	[−0.017; 0.135]
B–C gradient	44	0.035	[0.021; 0.049]	<0.001	0.365	<0.001	0.017	[0.010; 0.028]

Table 11. Annual SST trend statistics for the offshore, coastal, and gradient series.

Seasonal robust statistics further show that warming is concentrated mainly in winter and spring, whereas summer is weakly positive offshore and slightly negative at the coastal point. This seasonal behavior is consistent with the initial interpretation that summer nearshore SST may be moderated by upwelling or coastal mixing, although this hypothesis requires confirmation by independent upwelling indices, winds, chlorophyll-a, and in situ observations.

Series	Season	OLS slope	OLS p	MK p	Sen slope	Sen 95% CI
B (offshore)	DJF	0.148	0.022	0.020	0.156	[0.037; 0.269]
B (offshore)	MAM	0.163	0.002	0.003	0.168	[0.064; 0.266]
B (offshore)	JJA	0.012	0.835	0.777	0.019	[−0.119; 0.150]
B (offshore)	SON	0.076	0.239	0.373	0.066	[−0.076; 0.202]
C (coastal)	DJF	0.111	0.091	0.077	0.123	[−0.016; 0.245]
C (coastal)	MAM	0.147	0.005	0.006	0.155	[0.056; 0.243]
C (coastal)	JJA	−0.018	0.777	0.903	−0.008	[−0.146; 0.162]
C (coastal)	SON	0.022	0.746	0.840	0.014	[−0.126; 0.160]

Table 12. Seasonal robust trend statistics for offshore point B and coastal point C.

doi.org/10.32388/OYZ6H3.2

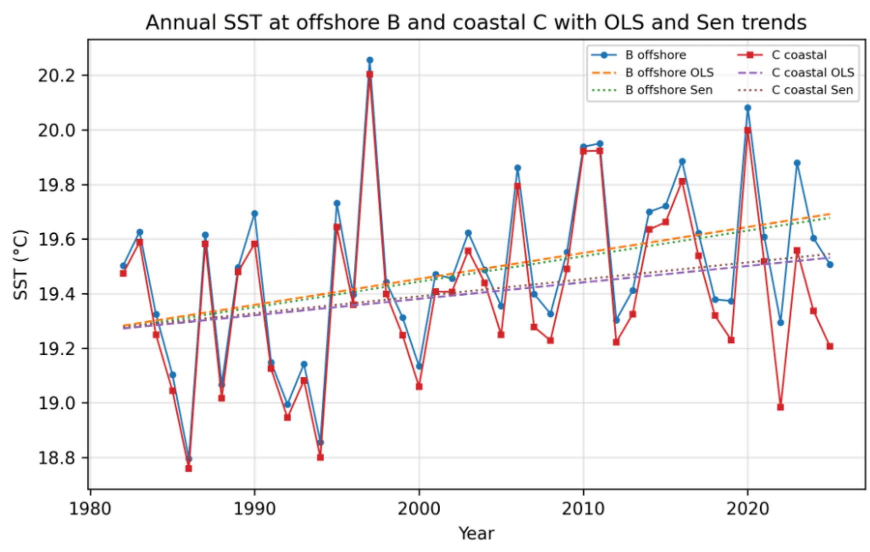

Figure 12. Annual SST at offshore point B and coastal point C with OLS and Sen trend lines.

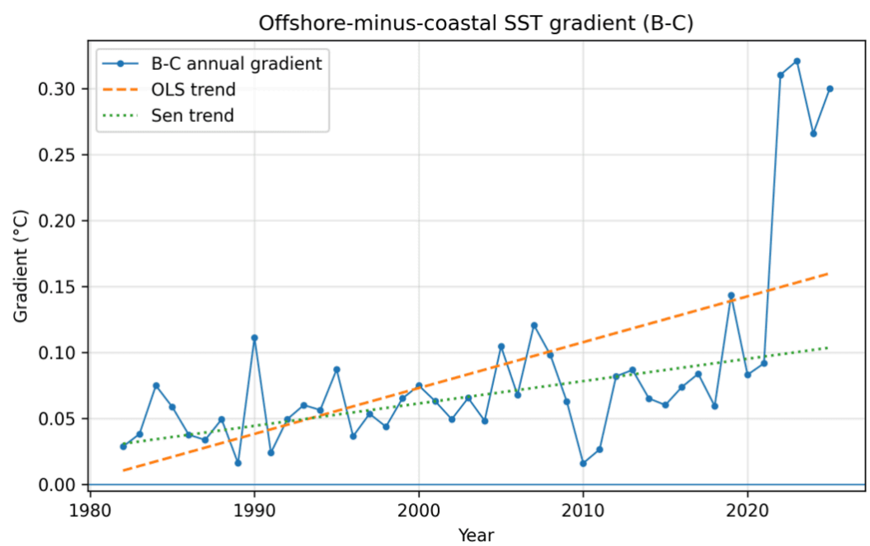

Figure 13. Offshore-minus-coastal SST gradient (B–C) with OLS and Sen trend lines.

doi.org/10.32388/OYZ6H3.2

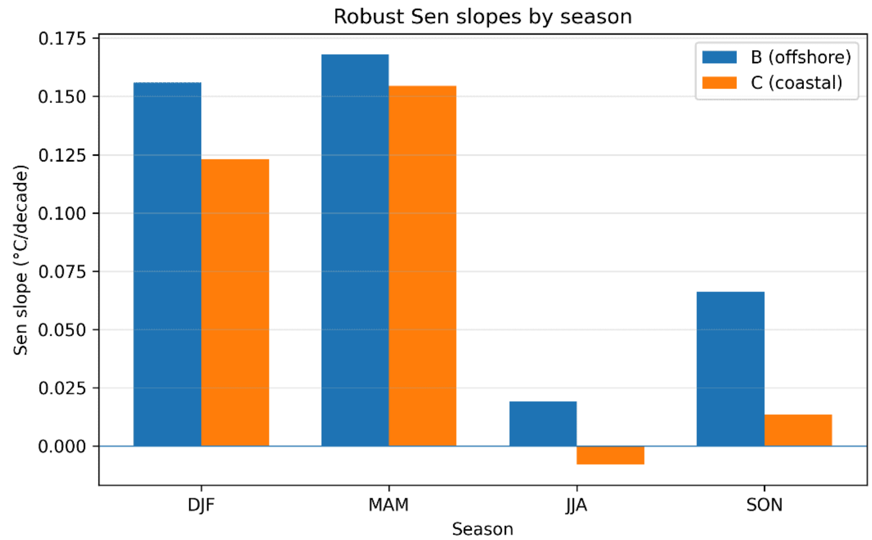

Figure 14. Robust Sen slopes by season for offshore point B and coastal point C.

5.8. MUR-based daily coastal-offshore thermal gradients

The MUR daily analysis for JJA 2016-2018 provided 276 daily values for each transect after retaining only June, July, and August. Individual dates were not selected arbitrarily. Daily offshore-minus-coastal gradients were first calculated for all available JJA days; then, instantaneous situations were classified according to the distribution of the regional index. This makes it possible to interpret the aggregated indicators in relation to actual daily SST contrasts.

The values reported below were obtained from daily calculations over 276 JJA days. The mean values, percentiles, and frequencies are summaries of daily instantaneous offshore-minus-coastal differences, not calculations made from a single seasonal mean.

Calculation lines used for Table 13 and Table 14:

$$\text{Mean } UI_B = \Sigma UI_B(d)/276 = 0.301^\circ\text{C}$$

$$\text{Mean } UI_D = \Sigma UI_D(d)/276 = 0.286^\circ\text{C}$$

$$\text{Mean } UI_F = \Sigma UI_F(d)/276 = 0.438^\circ\text{C}$$

$$\text{Frequency } UI_B > 0 = 237/276 \times 100 = 85.9\%$$

$$\text{Frequency } UI_D > 0 = 249/276 \times 100 = 90.2\%$$

$$\text{Frequency } UI_F > 0 = 246/276 \times 100 = 89.1\%$$

$$\text{Mean gradient } B - B' = 0.301/14.45 = 0.0208^\circ\text{C km}^{-1}$$

$$\text{Mean gradient } D - D' = 0.286/12.46 = 0.0230^\circ\text{C km}^{-1}$$

$$\text{Mean gradient } F - F' = 0.438/17.45 = 0.0251^\circ\text{C km}^{-1}$$

The 90th and 95th percentiles were calculated directly from the ranked daily UI values of each transect.

Example of an instantaneous calculation (August 15, 2020, used only to illustrate the formula):

$$UI_B = 21.756 - 21.514 = +0.242^\circ\text{C}$$

$$UI_D = 22.126 - 21.731 = +0.395^\circ\text{C}$$

$$UI_F = 22.442 - 21.702 = +0.740^\circ\text{C}$$

$$UI_{mean} = (0.242 + 0.395 + 0.740)/3 = +0.459^\circ\text{C}$$

Transect	N days	Mean UI (°C)	Median UI (°C)	P90 (°C)	P95 (°C)
B-B′	276	0.301	0.268	0.709	0.897
D-D′	276	0.286	0.220	0.662	0.819
F-F′	276	0.438	0.361	0.993	1.208

Table 13. Daily MUR coastal-offshore SST gradients during JJA 2016-2018: central tendency and high-percentile values.

Transect	Min (°C)	Max (°C)	Days UI > 0 (%)	Distance (km)	Mean gradient (°C/km)
B-B′	-0.270	1.276	85.9	14.45	0.0208
D-D′	-0.331	1.313	90.2	12.46	0.0230
F-F′	-0.455	1.985	89.1	17.45	0.0251

Table 14. Daily MUR coastal-offshore SST gradients during JJA 2016-2018: range, frequency, and normalized gradient.

The strongest mean coastal-cooling signal was observed along the F-F′ transect, with a mean offshore-minus-coastal difference of 0.438 °C and a 95th percentile of 1.208 °C. The B-B′ and D-D′ transects also showed persistent positive gradients, with mean values of 0.301 °C and 0.286 °C, respectively. Positive gradients occurred during 85.9% of days along B-B′, 90.2% along D-D′, and 89.1% along F-F′.

Calculation lines used for the regional index:

$$UI_{mean}(d) = [UI_B(d) + UI_D(d) + UI_F(d)]/3$$

$$\text{Mean } UI_{mean} = \Sigma UI_{mean}(d)/276 = 0.342^\circ\text{C}$$

$$\text{Frequency } UI_{mean} > 0 = 262/276 \times 100 = 94.9\%$$

$$\text{Frequency with at least two positive transects } = 254/276 \times 100 = 92.0\%$$

doi.org/10.32388/OYZ6H3.2

$$\text{Frequency with three positive transects } = 207/276 \times 100 = 75.0\%$$

Indicator	Value
Number of days	276
Mean UImean (°C)	0.342
Median UImean (°C)	0.283
P90 (°C)	0.686
P95 (°C)	0.875
Maximum (°C)	1.265
Days with UImean > 0 (%)	94.9
Days with at least two positive transects (%)	92.0
Days with three positive transects (%)	75.0

Table 15. Regional daily coastal-cooling index based on the three MUR transects during JJA 2016-2018.

The regional index was positive on 94.9% of days, and at least two of the three transects showed positive offshore-minus-coastal gradients on 92.0% of days. This spatial coherence supports the interpretation of a recurrent summer coastal-cooling signal during the analyzed period. The selected instantaneous situations were therefore not chosen arbitrarily; they were identified from the daily distribution of MUR-derived coastal-offshore gradients using percentile and spatial-coherence criteria.

Situation type	Date	UI B-B′ (°C)	UI D-D′ (°C)	UI F-F′ (°C)	UI mean (°C)	Spatial coherence
Strong coastal cooling	2018-06-10	1.276	1.313	1.206	1.265	3 positive transects
Median situation	2017-07-24	0.288	0.208	0.364	0.287	3 positive transects
Weak/inverse situation	2017-08-08	-0.048	-0.044	-0.304	-0.132	0 positive transects

Table 16. Examples of objectively selected instantaneous MUR SST situations during JJA 2016-2018.

These examples were not selected manually. They were selected from the daily distribution of UI_mean: the strong situation corresponds to the upper tail of the daily distribution, the median situation is close to P50, and the weak/inverse situation corresponds to a day with negative gradients in all three transects. This approach makes the interpretation of the mean values more transparent by showing the instantaneous daily situations from which the aggregated statistics were derived.

6. Discussion

6.1. A warming signal with a non-uniform spatial structure

The NOAA time series indicate a positive annual SST trend at all three points over 1982–2025, confirming a background warming signal in the El Jadida marine region. However, the intensity of the signal differs spatially. Point D shows the strongest trend and the largest increase between the early and recent decades, whereas the coastal point C shows the weakest annual warming. This result is important because the coastal zone relevant to Gelidium should not be treated as thermally identical to the offshore domain. It also illustrates the value of combining long-term regional products such as NOAA OISST v2.1 with higher-resolution coastal products such as Copernicus and MUR SST fields.

The stronger trend at D is scientifically interesting but should be interpreted with caution. It may reflect spatial heterogeneity within the offshore thermal field, a local front-related behavior, or differences in the seasonal exposure of the outer shelf. However, the present SST analysis does not allow a direct conclusion on the displacement of the upwelling front. This point is therefore treated as a hypothesis-generating observation rather than a demonstrated mechanism.

6.2. Upwelling as a possible moderator of summer warming

The seasonal decomposition of the NOAA series shows that warming is strongest in spring and weakest in summer. At point C, the summer trend is slightly negative. This pattern is compatible with a local moderating effect of seasonal coastal cooling, but it does not prove that upwelling has intensified. The complementary MUR daily analysis supports this interpretation by showing recurrent positive offshore-minus-coastal gradients along the three paired transects during JJA 2016–2018. The regional MUR index was positive in most daily situations, and at least two transects were positive on 92.0% of days. This indicates that the shallow coastal domain near the 20 m isobath was generally cooler than the offshore reference points during the analyzed summer period.

6.3. Biological and ecological relevance of SST for Gelidium populations

The present study focuses on one environmental component only: sea surface temperature. It does not aim to provide a direct biological assessment of Gelidium beds in the El Jadida region, nor does it attempt to establish a causal relationship between SST variability and changes in local Gelidium biomass, cover, reproduction, or harvesting yield. Such a causal interpretation would require in situ ecological monitoring, including repeated surveys of Gelidium abundance, population structure, recruitment, thallus condition, substrate characteristics, harvesting pressure, and associated environmental variables. The objective of this work is more limited but nevertheless relevant: to characterize the long-term marine thermal context in which Gelidium populations occur along an economically and ecologically important Moroccan Atlantic coastal sector.

The link between this SST analysis and Gelidium ecology is supported by several biological and ecological studies showing that Gelidium species are not indifferent to their thermal environment. The genus Gelidium includes perennial red algae attached to rocky substrates, whose persistence depends on the maintenance of suitable benthic habitats, vegetative propagation, regeneration, and recruitment processes, as described in the biological synthesis of Santelices[8]. In the Atlantic context, Gelidium corneum is widely recognized as a valuable agarophyte and as a structurally important red seaweed associated with rocky coastal habitats, including the Atlantic coasts of Morocco, Portugal, Spain, and France[4][9].

Temperature is particularly relevant because it can influence physiological and demographic processes in macroalgae, including growth, respiration, photosynthetic performance, reproduction, recruitment, and recovery after disturbance. For Gelidium corneum, experimental evidence is especially important. Sainz-Villegas et al.[10] examined the combined effects of temperature and irradiance on vegetative propagation, including re-attachment capacity and the survival of re-attached fragments. Their results showed that both temperature and irradiance significantly affect the re-attachment process, with more favorable responses around 20 °C under low irradiance conditions, whereas less favorable thermal-light combinations may reduce the development of rhizoids and attachment structures. This demonstrates that temperature is not only a descriptive oceanographic variable but a factor that may affect biological processes involved in the maintenance and regeneration of Gelidium populations. Additional field-based evidence supports this interpretation: Sánchez-Astráin et al.[14] assessed newly sprouted shoots of Gelidium corneum and reported that vegetative propagation is an important recovery mechanism, while elevated mean summer seawater temperatures above about 22 °C may slow frond elongation. Together, these studies indicate that SST changes are ecologically relevant because they may affect re-attachment, rhizoid development, shoot elongation, and post-disturbance recovery, even though these biological responses remain to be tested directly in El Jadida.

On this basis, the following conceptual pathways can be proposed for future testing in El Jadida: (i) warmer spring conditions may modify growth and the timing of seasonal recovery; (ii) warmer autumn conditions may affect post-summer regeneration and resilience; (iii) summer upwelling may buffer nearshore thermal stress at the coastal point C; (iv) changes in upwelling intensity may alter both temperature and nutrient supply; and (v) thermal variability may interact with irradiance, hydrodynamics, sedimentation, and harvesting pressure to influence recruitment, re-attachment, and canopy persistence. These pathways are hypotheses generated from the thermal analysis and from the literature; they should not be interpreted as demonstrated biological impacts for El Jadida.

Recent distributional and community-level studies further support a multi-driver interpretation of Gelidium responses. Sánchez-Astráin et al.[15] used Gelidium corneum as a case study for phenotypic plasticity in macroalgal distribution, showing the relevance of local environmental gradients when interpreting distributional patterns. Guinda et al.[16] analyzed subtidal macroalgal shifts in a transitional northeastern Atlantic coastal region and highlighted the role of extreme events. These studies reinforce the view that SST should be treated as one component of a broader ecological pathway, interacting with irradiance, wave exposure, disturbance regime, nutrient availability, and habitat condition.

Therefore, the SST signal described for El Jadida should be interpreted as an environmental context indicator rather than direct biological evidence of Gelidium decline. The relatively weak summer warming at the coastal point C may reflect the moderating influence of local upwelling, which could partly buffer nearshore habitats during the warm season. However, the observed warming during spring and autumn remains ecologically relevant because these transitional seasons may influence growth, recovery, reproductive timing, recruitment, and competitive interactions within rocky-shore macroalgal communities. The response of Gelidium to future warming will likely depend on the interaction between SST, upwelling intensity, nutrient supply, irradiance, water movement, sedimentation, rocky substrate quality, and harvesting pressure.

In this sense, the present study should be considered a first thermal baseline for the El Jadida-Jorf Lasfar coastal sector. It provides a regional-scale assessment of the marine thermal signal over the period 1982–2025, while highlighting the need for future work combining satellite-derived SST, in situ temperature measurements, and biological monitoring of Gelidium beds. This approach would allow future studies to move from thermal context analysis toward a more complete understanding of the ecological vulnerability and resilience of Moroccan Gelidium populations.

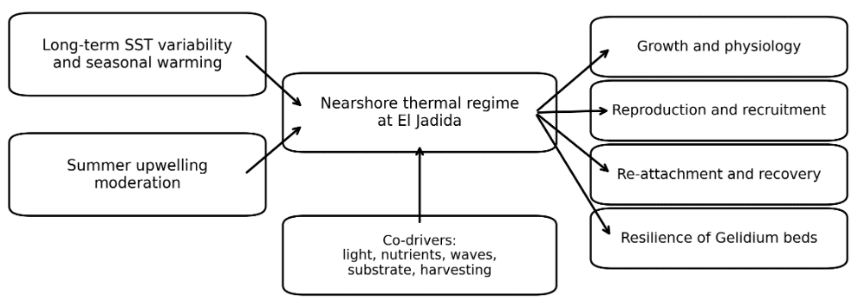

Figure 15. Conceptual pathway linking long-term SST variability, summer coastal cooling, and ecological response components relevant to Gelidium habitats.

6.4. Comparison with Spain, Portugal, and the Canary Islands

Comparison with the Iberian Peninsula and the Canary Islands is justified because Morocco, Portugal, and Spain belong to the historical Atlantic Gelidium exploitation area for agar production. McHugh[4] identifies Morocco, Portugal, and Spain among countries where harvested Gelidium has supplied local agar producers. Santos and Melo[5] also emphasized the importance and vulnerability of Gelidium resources in the global technical agar supply chain.

According to Borja et al.[17], the Basque coast of northern Spain experienced a marked decline in Gelidium corneum biomass, from about 12,000 t to 1,900 t over approximately two decades, with several environmental hypotheses including sea surface temperature, wave conditions, irradiance, and nutrient changes. Mugerza et al.[18] also documented decades of biomass loss in shallow rocky subtidal vegetation in the southeastern Bay of Biscay. Ramos et al. [19] showed that intertidal macroalgal communities along the northern coast of Spain have undergone distributional changes along environmental gradients. In the Canary Islands, Alfonso et al.[20] reported that more than 90% of populations of the endemic Gelidium canariense declined over three decades and that the cover of Gelidium canariense and Gelidium arbuscula decreased significantly with increasing SST and air temperature. These examples do not demonstrate that the same trajectory is occurring in El Jadida, but they show that Gelidium-related issues in El Jadida should be considered within a broader Atlantic context of climate-related macroalgal change.

6.5. Limitations and monitoring needs

This study has several limitations. First, NOAA OISST is appropriate for long-term climate analysis, but its 0.25° grid is coarse for nearshore ecological interpretation. Second, the Copernicus analysis is limited to two months in 2025 and is used only as cold- and warm-season spatial snapshots. Third, the MUR analysis improves the spatial interpretation of summer coastal cooling, but it covers only JJA 2016–2018 in the present version and remains a surface thermal proxy. Fourth, none of the satellite products provides direct near-bottom temperature measurements within Gelidium beds. Fifth, SST alone cannot determine the ecological status of Gelidium populations. Field data on biomass, cover, recruitment, substrate condition, harvesting pressure, turbidity, nutrients, wave exposure, wind forcing, currents, and local upwelling indicators are required to establish a robust ecological diagnosis.

Future work should combine satellite SST, MUR-based coastal-offshore gradients, wind stress or Ekman transport, chlorophyll-a, in situ coastal temperature loggers, seasonal Gelidium surveys, nutrient measurements, and harvest statistics. Such an integrated approach would make it possible to distinguish between climate-driven thermal change, local habitat degradation, and direct exploitation pressure, while keeping the present analysis in its appropriate scope: a climate-oriented thermal baseline based on SST and surface coastal-cooling indicators.

6.6. Relevance for future monitoring and coastal management

The results can support future monitoring without being formulated as direct management prescriptions. The El Jadida–Jorf Lasfar coastal sector may be considered a useful sentinel area for observing the interaction between SST variability, upwelling modulation, and rocky-shore agarophyte habitats. A cautious monitoring framework could combine satellite-derived SST, in situ temperature loggers, periodic Gelidium bed surveys, simple upwelling indicators, nutrient measurements, habitat condition assessment, and harvesting information. Such a framework would make it possible to evaluate whether the thermal patterns identified here correspond to biological changes in Gelidium beds or whether local habitat and harvesting factors remain the dominant drivers.

6.7. Interpretation of Gelidium relevance after statistical analysis

The statistical results improve the physical basis of the analysis, but they do not transform the study into a direct population assessment of Gelidium. The ecological interpretation is therefore framed as a relevance analysis rather than a causal demonstration. The El Jadida region is ecologically and socioeconomically linked to Gelidium resources, and SST is one of the environmental variables that can affect habitat suitability, phenology, productivity, and stress exposure in macroalgal systems. However, the observed SST trends must be combined with field data on Gelidium distribution, biomass, recruitment, harvesting pressure, substrate conditions, nutrients, turbidity, and hydrodynamics before direct biological responses can be inferred. This cautious framing preserves the ecological relevance of Gelidium while avoiding over-interpretation.

6.8. Climate-change integration in fisheries and algal resource management plans

The analysis also highlights a broader issue for coastal resource planning. The relevance of this study is not limited to a narrow causal claim between SST and Gelidium. Rather, it lies in showing that long-term marine climate information can and should be incorporated into the diagnosis of harvested coastal resources. In the case of El Jadida, Gelidium represents an important agarophyte resource with ecological, economic, and social significance for coastal communities. Ignoring the climate component in management planning would leave such resources exposed to environmental changes that may alter productivity, recovery capacity, accessibility, and long-term sustainability.

This point extends beyond Gelidium. Climate-change integration should concern fisheries management plans as a whole, including algae, shellfish, demersal species, pelagic species, and other coastal resources. Management plans that rely only on historical exploitation patterns, static zoning, or short-term biological indicators may underestimate climate-driven shifts in temperature, upwelling intensity, phenology, habitat suitability, and ecosystem productivity. A climate-informed approach would combine conventional stock or resource assessment with physical indicators such as SST trends, marine heat anomalies, seasonal warming, upwelling indices, and coastal productivity indicators.

Accordingly, the present manuscript is positioned as a first modeling-based environmental screening exercise. It does not replace field surveys of Gelidium beds or dedicated population monitoring, but it provides a reproducible physical baseline that can inform future algal and fisheries management plans. The value of the study is therefore both scientific and operational: it identifies where the marine climate signal is strong or seasonally moderated and demonstrates why this signal should be explicitly considered in future planning for Gelidium and for coastal fisheries more generally.

7. Conclusion

The analysis of NOAA OISST data for 1982–2025 reveals a detectable warming signal in the El Jadida marine region, but the signal is spatially and seasonally heterogeneous. Annual warming is strongest at the offshore/outer-shelf point D, intermediate at the offshore reference point B, and weakest at the coastal point C. Spring is the season with the strongest warming, whereas summer remains comparatively stable, especially near the coast. The weak summer warming at C

doi.org/10.32388/OYZ6H3.2

is compatible with the hypothesis that coastal cooling processes may moderate summer thermal exposure in the shallow coastal domain.

The complementary Copernicus extraction for February and August 2025 confirms a local gradient between the targeted coastal point and the offshore points, with C remaining cooler, especially in August. The MUR daily analysis for JJA 2016-2018 further shows that shallow coastal points near the 20 m isobath were generally cooler than their offshore counterparts, with positive gradients in most daily situations. Together, these results support the interpretation of recurrent summer coastal cooling along the El Jadida-Jorf Lasfar sector. For Gelidium populations, the results provide a climate-relevant environmental baseline, but not a direct ecological diagnosis. The work should therefore be viewed as a first climate diagnostic assessment to support future field-based ecological studies and the integration of climate-change indicators into algal and fisheries management plans.

Abbreviations

The following abbreviations are used in the manuscript.

doi.org/10.32388/OYZ6H3.2

Abbreviation	Meaning
B, C, D	NOAA-based study point labels used for the regional coastal-offshore SST analysis.
B–B′, D–D′, F–F′	Paired MUR coastal-offshore transects used for the high-resolution daily gradient analysis.
CI	Confidence interval.
DJF	December-January-February winter season.
DOISST	Daily Optimum Interpolation Sea Surface Temperature.
FAO	Food and Agriculture Organization of the United Nations.
G	Distance-normalized coastal-offshore SST gradient, expressed in °C km^{-1}.
HS	Harmonized System commodity classification.
JJA	June-July-August summer season.
L4	Level-4 gridded and gap-free satellite-derived product.
MAM	March-April-May spring season.
MK	Mann-Kendall non-parametric trend test.
MUR	Multi-scale Ultra-high Resolution Sea Surface Temperature Analysis.
NASA	National Aeronautics and Space Administration.
NOAA	National Oceanic and Atmospheric Administration.
OISST	Optimum Interpolation Sea Surface Temperature.
OLS	Ordinary least squares regression.
P50, P90, P95	50th, 90th and 95th percentiles.
PO.DAAC	Physical Oceanography Distributed Active Archive Center.
R^2	Coefficient of determination.
SON	September-October-November autumn season.
SST	Sea surface temperature.
UI	Offshore-minus-coastal SST difference used as a surface thermal coastal-cooling proxy.
UImean	Mean daily coastal-cooling index calculated from UIB, UID and UIF.
UN Comtrade	United Nations international trade statistics database.
USD	United States dollar.
WITS	World Integrated Trade Solution database.

Statements and Declarations

Funding

No external funding was reported for this work.

Potential Competing Interests

The authors declare no competing interests.

Ethics

This study did not involve human participants, animals, clinical data or experimental manipulation. Ethical approval was therefore not applicable.

Data Availability

The SST data used in this study are publicly available from NOAA OISST v2.1, the Copernicus Marine Service product SST_ATL_SST_L4_REP_OBSERVATIONS_010_026 and the MUR/JPL SST product. The processed NOAA monthly series, Copernicus extraction table, MUR JJA 2016-2018 daily coastal-offshore gradient file, trend calculation sheets and scripts used for the tables and figures are provided as supplementary material.

Author Contributions

Abdellatif ORBI: conceptualization, oceanographic interpretation, study design, writing and supervision. Jalal ANNACHAT: data extraction support, mapping/processing support and technical contribution. Both authors reviewed and approved the manuscript before submission.

Use of Generative AI

Language editing, translation support and manuscript formatting assistance were supported by AI tools. The authors remain fully responsible for the scientific content, data interpretation, accuracy of results, references, and final manuscript.

Acknowledgments

The authors acknowledge the availability of NOAA, Copernicus Marine and MUR/JPL SST data products used in this analysis.

References

1. ^*Bograd SJ, Jacox MG, Hazen EL, Lovecchio E, Montes I, Pozo Buil M, Shannon LJ, Sydeman WJ, Rykaczewski RR. (2023). "Climate Change Impacts on Eastern Boundary Upwelling Systems." Annu Rev Mar Sci.* ***15****(1):303328. doi:10.1146/annurev-marine-032122-021945.*
2. ^*Santos F, deCastro M, Gmez-Gesteira M, lvarez I. (2012). "Differences in Coastal and Oceanic SST Warming Rates Along the Canary Upwelling Ecosystem From 1982 to 2010." Cont Shelf Res.* ***47****:16. doi:10.1016/j.csr.2012.07.023.*
3. ^*Belmajdoub H, Minaoui K, El Aouni A, Hilmi K, Saadane R, Chehri A. (2023). "A New Upwelling Index for the Moroccan Atlantic Coast for the Period Between 198 22021." Remote Sens.* ***15****(14):3459. doi:10.3390/rs15143459.*
4. a, b, c*McHugh DJ. (2003). A Guide to the Seaweed Industry (FAO Fisheries Technical Paper No. 441). Food and Agriculture Organization of the United Nations. ISBN 9251049580.*
5. a, b*Santos R, Melo RA. (2018). "Global Shortage of Technical Agars: Back to Basics (Resource Management)." J Appl Phycol.* ***30****(4):24632473. doi:10.1007/s10811-018-1425-2.*

6. ^World Bank. (2023). "Morocco Agar-Agar Exports by Country | 2023 | Data." World Integrated Trade Solution. https://wits.worldbank.org/trade/comtrade/en/country/MAR/year/2023/tradeflow/Exports/partner/ALL/product/130231.
7. ^Ministry of Industry and Trade, Kingdom of Morocco. (2023). "Avis aux Exportateurs des Algues Brutes et Agar Agar - 2022-2023 [Notice to Exporters of Raw Algae and Agar Agar - 2022-2023]." https://mcinet.gov.ma/sites/default/files/documents/Avis%20aux%20exportateurs%20des%20Algues%20brutes%20et%20Agar%20agar%20-%202022-2023 0.pdf.
8. a, bSantelices B. (1988). Synopsis of Biological Data on the Seaweed Genera Gelidium and Pterocladia (Rhodophyta) (FAO Fisheries Synopsis No. 145). Food and Agriculture Organization of the United Nations. ISBN 925102717X.
9. a, bMouga T, Fernandes IB. (2022). "The Red Seaweed Giant Gelidium (Gelidium corneum) for New Bio-Based Materials in a Circular Economy Framework." Earth. **3**(3):788813. doi:10.3390/earth3030045.
10. a, bSainz-Villegas S, Snchez-Astrin B, Puente A, Juanes JA. (2023). "Characterization of Gelidium corneum's (Florideophyceae, Rhodophyta) Vegetative Propagation Process Under Increasing Levels of Temperature and Irradiance." Mar Environ Res. **187**:105966. PMID 36996639.
11. ^INRH. (2015). Diagnostic de la Rcolte et de la Valorisation des Algues Marines [Diagnosis of the Harvesting and Valorization of Marine Algae]. Casablanca: Institut National de Recherche Halieutique.
12. ^NOAA National Centers for Environmental Information. (n.d.). "Optimum Interpolation Sea Surface Temperature (OISST). Version 2.1." https://www.ncei.noaa.gov/products/optimum-interpolation-sst.
13. ^Huang B, Liu C, Banzon VF, Freeman E, Graham G, Hankins B, Smith TM, Zhang H-M. (2021). "Improvements of the Daily Optimum Interpolation Sea Surface Temperature (DOISST) Version 2.1." J Clim. **34**(8):29232939. doi:10.1175/JCLI-D-20-0166.1.
14. ^Snchez-Astrin B, Sainz-Villegas S, Guinda X, Fernndez de la Hoz C, Juanes JA. (2024). "Assessment of the Growth Capacity of Newly Sprouted Shoots of Gelidium corneum (Florideophyceae, Rhodophyta) Through Field-Based Experiments." Mar Environ Res. **202**:106781. doi:10.1016/j.marenvres.2024.106781.
15. ^Snchez-Astrin B, Sainz-Villegas S, Guinda X, Fernndez de la Hoz C, Juanes JA. (2025). "Phenotypic Plasticity in Macroalgal Distribution: A Case Study on Gelidium corneum (Florideophyceae, Rhodophyta)." Sci Total Environ. **1008**:181024. doi:10.1016/j.scitotenv.2025.181024.
16. ^Guinda X, Ramos E, Fernndez de la Hoz C, Puente A, Juanes JA. (2026). "Subtidal Macroalgae Shifts in a Key Transitional Coastal Region: The Role of Extreme Events." Mar Environ Res. **215**:107808. doi:10.1016/j.marenvres.2025.107808.
17. ^Borja A, Chust G, Fontn A, Garmendia JM, Uyarra MC. (2018). "Long-Term Decline of the Canopy-Forming Algae Gelidium corneum, Associated to Extreme Wave Events and Reduced Sunlight Hours, in the Southeastern Bay of Biscay." Estuar Coast Shelf Sci. **205**:152160. doi:10.1016/j.ecss.2018.03.016.
18. ^Muguerza N, Dez I, Quintano E, Gorostiaga JM. (2022). "Decades of Biomass Loss in the Shallow Rocky Subtidal Vegetation of the South-Eastern Bay of Biscay." Mar Biodivers. **52**:28. doi:10.1007/s12526-022-01268-2.
19. ^Ramos E, Guinda X, Puente A, Fernndez de la Hoz C, Juanes JA. (2020). "Changes in the Distribution of Intertidal Macroalgae Along a Longitudinal Gradient in the Northern Coast of Spain." Mar Environ Res. **157**:104930. doi:10.1016/j.marenvres.2020.104930.

20. ^*Alfonso B, Hernndez JC, Sangil C, Martn L, Expsito FJ, Daz JP, Sansn M. (2021). "Fast Climatic Changes Place an Endemic Canary Island Macroalga at Extinction Risk." Reg Environ Change. **21**:113. doi:10.1007/s10113-021-01828-5.*

Declarations

Funding: No specific funding was received for this work.
Potential competing interests: No potential competing interests to declare.